Solvation Dynamics in Ionic Liquid Swollen P123 Triblock Copolymer Micelle: A Femtosecond Excitation Wavelength Dependence Study

Aniruddha Adhikari, Shantanu Dey, Dibyendu Kumar Das, Ujjwal Mandal, Subhadip Ghosh, and Kankan Bhattacharyya*

Department of Physical Chemistry, Indian Association for the Cultivation of Science, Jadavpur, Kolkata 700 032, India

Received: December 19, 2007; Revised Manuscript Received: February 25, 2008

Femtosecond solvation dynamics of coumarin 480 (C480) in a mixed micelle is reported. The mixed micelle consists of a triblock copolymer $(PEO)_{20}-(PPO)_{70}-(PEO)_{20}$ (Pluronic P123) and an ionic liquid (IL), 1-pentyl-3-methylimidazolium tetrafluoroborate ([pmim][BF_4]). At a low concentration (0.3 M), the sparingly water soluble IL ([pmim][BF_4]) penetrates the hydrophobic PPO core of the P123 micelles. Thus emission maximum of C480 in the core (accessed at $\lambda_{ex} = 375$ nm) in 0.3 M IL is red-shifted by 8 nm from that in its absence and the red edge excitation shift (REES) is large (19 ± 1 nm). At a high concentration (0.9 M), the ionic liquid [pmim][BF_4] invades both the core and corona region and the mixed micelle exhibits very small REES (3 ± 1 nm). Anisotropy decay and solvation dynamics in different regions of the mixed micelle are studied by variation of excitation wavelength (λ_{ex}). In P123 micelle, the average rotational time ($\langle\tau_{rot}\rangle$) is 2800 ps in the core (at $\lambda_{ex} = 375$ nm) and 1350 ps in the corona region (at $\lambda_{ex} = 435$ nm). In 0.3 M [pmim][BF_4], $\langle\tau_{rot}\rangle$ at the core of the mixed micelle decreases to 1950 ps while that in the corona remains unaffected. In 0.9 M IL, both the core and corona ($\lambda_{ex} = 375$ and 435 nm) exhibit similar and short $\langle\tau_{rot}\rangle \sim 600$ ps. In 0.3 M IL, solvation dynamics in the core region ($\lambda_{ex} = 375$ nm) of P123 micelle is about 2 times faster than in its absence. In 0.3 M IL, solvation dynamics in the corona region ($\lambda_{ex} = 435$ nm) is ~100 times faster than that in the core. In 0.9 M IL, the solvation dynamics in the core and in the corona is, respectively, ~9 times and 4 times faster than that in 0.3 M IL.

1. Introduction

Room-temperature ionic liquids (RTILs) have received vigorous recent attention as environmentally benign ("green"), designer solvents and catalysts for many organic reactions.[1–3] In a RTIL, the steric hindrance of the bulky ions frustrates formation of the crystal and thus lowers the melting point while the interionic attractions increase the boiling point. This keeps a RTIL in the liquid state over a wide range of temperature. The polarity and solvation properties of the RTILs are addressed in several recent works. Solvation dynamics in a RTIL occurs in a slow (nanosecond) time scale along with a fast subpicosecond component.[4–6] Recent computer simulations suggest that solvation dynamics in a RTIL involves collective motion of the cation and the anion.[3] Most recently, several groups reported nanoscale organization in RTILs with clear segregation of the polar (ions) and nonpolar (alkyl side chain) domains. Such organization has been predicted in computer simulations.[1a,7] Subsequently, X-ray diffraction[8a] and optical heterodyne Kerr spectroscopy[8b] confirmed the presence of aggregates of size 13−27 Å in RTILs with alkyl chains containing four to ten carbon atoms. Raman spectroscopy also indicates formation of such nanostructures.[1c,9] Recently, we have demonstrated that a neat RTIL is heterogeneous and solvation dynamics depends on location of the probe.[10]

Self-assembly of amphiphilic molecules in RTILs is a recent topic of research. Petrich and co-workers studied solvation dynamics in neat amphiphilic RTILs and their micelles in water.[11a,b] Sarkar and co-workers studied a RTIL/brij mixed micelle using picosecond spectroscopy.[11c–e] Gao et al. reported formation of a microemulsion containing a nanosized pool of ionic liquid using dynamic light scattering (DLS).[12a,b] Eastoe et al. carefully examined the structure of the same system using small-angle neutron scattering (SANS).[12c] From ultrafast vibrational relaxation studies in ionic liquid microemulsions, Owtrusky and co-workers concluded that the RTIL microemulsions are more polar than the neat RTILs.[13] We have recently probed different regions of such a RTIL microemulsion using femtosecond spectroscopy.[10]

In the present work, we report on interaction of the triblock copolymer $(PEO)_{20}-(PPO)_{70}-(PEO)_{20}$ (Pluronic P123) with an ionic liquid, 1-pentyl-3-methylimidazolium tetrafluoroborate ([pmim][BF_4]). Liu et al. investigated the effect of addition of an ionic liquid, 1-butyl-3-methylimidazolium bromide ([bmim][Br]) on the aggregation of a triblock copolymer, $(PEO)_{27}-(PPO)_{61}-(PEO)_{27}$ (Pluronic P104).[14a] They showed that the size of P104 micelles gradually increases on addition of [bmim][Br].[14a] The ionic liquid [pmim][BF_4] is sparingly soluble in water (solubility ~0.7 M at 20 °C).[14b,c] In the presence of P123 as much as 0.9 M [pmim][BF_4] dissolves in water. The sparingly soluble ionic liquid penetrates the P123 micelles. The structure of a P123 micelle has been thoroughly investigated using SANS, small-angle X-ray scattering (SAXS), and NMR.[15] According to SANS studies, a P123 micelle consists of a hydrophobic core (PPO block) with a radius of 4.8 nm and a hydrophilic corona (PEO block) of thickness 4.6 nm (Scheme 1A) so that the diameter is ~18 nm.[15]

* Corresponding author. E-mail: pckb@mahendra.iacs.res.in.

10.1021/jp7118857 CCC: $40.75
Published on Web 04/24/2008

SCHEME 1: Schematic Representation of (A) P123 Micelle, (B) Coumarin 480 (C480), and (C) [pmim][BF_4]

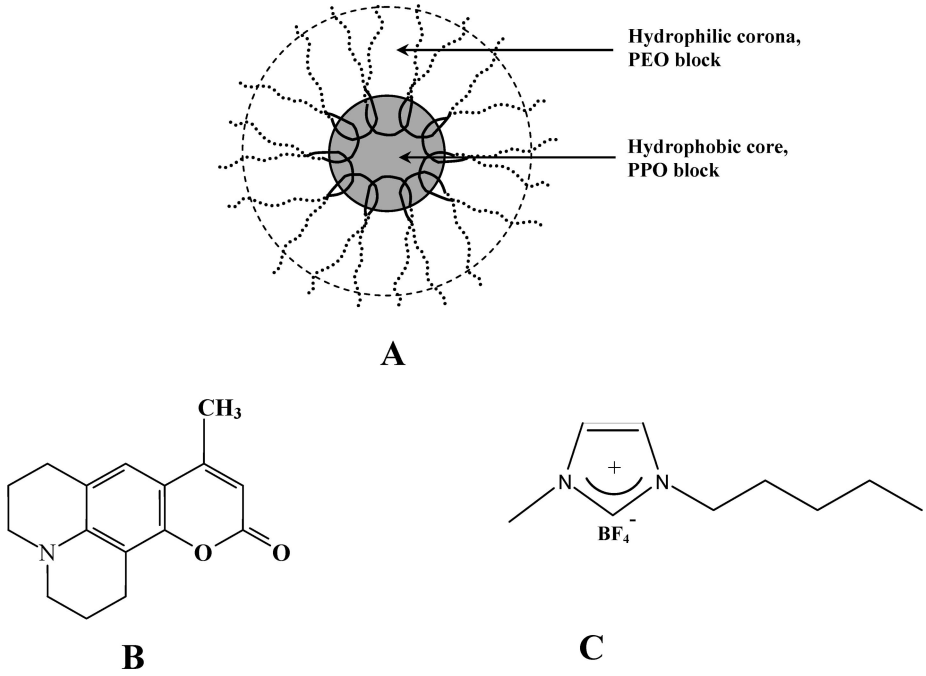

TABLE 1: DLS Data on Diameters of 5 wt % P123 Micelle Containing [pmim][BF_4]

concn of IL (M)	mean diameter (nm)	polydispersity index
0	18.2	0.15
0.3	21.0	0.23
0.6	15.7	0.12
0.9	13.5	0.30

Several groups recently reported on solvation dynamics and anisotropy decay in P123 micelles.[16] In this work, we report on the structure and solvation dynamics in the ionic liquid ([pmim][BF_4]) swollen P123 micelle. We have used DLS to study the structure of the IL swollen P123 micelle. Finally, we have applied femtosecond upconversion to study solvation dynamics in different regions of the P123−[pmim][BF_4] aggregate. A simple method to probe different regions is to utilize the polarity dependence of the probe. The absorption maximum of a solvatochromic probe depends on local polarity and thus varies from one region to another. Thus, by varying the excitation wavelength (λ_{ex}), it is possible to excite the probe selectively at different locations. This is the basis of the so-called red edge excitation shift (REES) which is observed in many organized assemblies.[17] Recently, using λ_{ex} dependence, we have studied solvation dynamics in different regions of many organized assemblies. Such λ_{ex} dependence has been observed in a microemulsion,[18a] a lipid vesicle,[18b] a micelle (triblock copolymer, P123),[16d] P123−SDS aggregate,[18c] and P123 gel.[18d] In the present work, we have used the solvatochromic dye coumarin 480 (C480) as a fluorescent probe.

2. Experimental Section

The triblock copolymer Pluronic P123 (P123) was a gift from BASF Corp. and was used without further purification. Laser-grade coumarin 480 (C480, Exciton, Scheme 1B) was used as received. Sodium tetrafluoroborate (98%, Aldrich), 1-methylimidazole (99%, Aldrich), and 1-bromopentane (99%, Aldrich) were used for the synthesis of the RTIL. Acetonitrile (Merck) was distilled over P_2O_5 and dichloromethane (Merck) was used as received. Diethyl ether (Merck) was distilled over KOH.

The RTIL, [pmim][Br], was prepared from 1-methylimidazole and 1-bromopentane following the sonochemical route.[19a] Pure [pmim][BF_4] (Scheme 1C) was obtained through the metathesis of [pmim][Br] with $NaBF_4$ in dry acetonitrile under argon

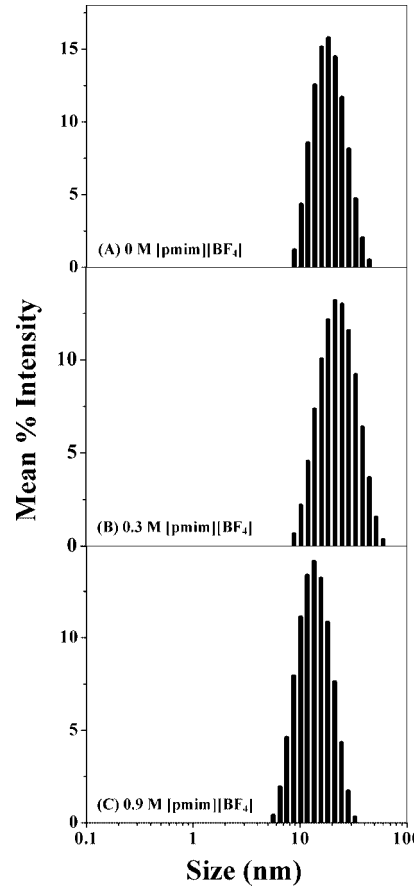

Figure 1. Size distribution of the droplets (measured by dynamic light scattering) in P123−[pmim][BF_4] aggregate in the presence of (A) 0 M [pmim][BF_4], (B) 0.3 M [pmim][BF_4], and (C) 0.9 M [pmim][BF_4].

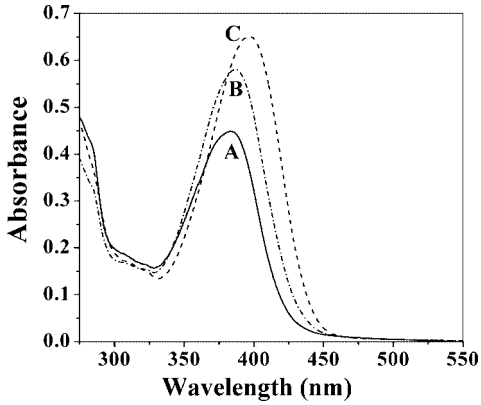

Figure 2. Absorption spectra of C480 in (A) 5 wt % P123 (—) and in the presence of (B) 0.3 M [pmim][BF_4] (—•—), and (C) 0.9 M [pmim][BF_4] (---).

TABLE 2: λ_{ex} Dependence of λ_{em}^{max} of C480 in 5 wt % P123 in the Presence of [pmim][BF_4]

	λ_{em}^{max} (nm)		
	[pmim][BF_4]		
λ_{ex} (nm)	0.3 M	0.9 M	water
375	463	477	489
405	470	478	489
435	478	479	489

atmosphere at room temperature.[19b,c] For purification, the raw [pmim][BF_4] was diluted with dichloromethane and filtered a couple of times through a silica gel column. The filtrate was treated with activated charcoal in an inert atmosphere for 48 h to remove any possible trace of color. After removal of dicholoromethane in a rotary evaporator, [pmim][BF_4] was repeatedly washed with dry diethyl ether to yield the RTIL in the form of a colorless, viscous liquid.

The copolymer solution was prepared by stirring the proper amount of the copolymer (P123) with 100 mL of water for 4−5 h at room temperature in a sealed container. We used 5 wt % P123 (~8.7 mM). All experiments were done at room temperature (~20 °C). The steady state absorption and emission spectra were recorded with a Shimadzu UV-2401 spectrophotometer and a Spex FluoroMax-3 spectrofluorimeter, respectively.

In our femtosecond upconversion setup (FOG 100, CDP) the sample was excited at 375, 405, and 435 nm, respectively, using the second harmonic of a mode-locked Ti:sapphire laser (Tsunami, Spectra Physics), pumped by a 5 W Millennia (Spectra Physics). In order to generate the second harmonic, we used a nonlinear crystal (1 mm BBO, $\theta = 25°$, $\varphi = 90°$). The fluorescence emitted from the sample was upconverted in a nonlinear crystal (0.5 mm BBO, $\theta = 38°$, $\varphi = 90°$) using the fundamental beam as a gate pulse. The upconverted light is dispersed in a monochromator and detected using photon-counting electronics. A cross-correlation function obtained using the Raman scattering from ethanol displayed a full width at half-maximum (fwhm) of 350 fs. The femtosecond transients were fitted using a Gaussian shape for the exciting pulse.

The femtosecond transients are fitted keeping the long picosecond components fixed. To determine the picosecond components, the samples were excited at 375, 405, and 435 nm using picosecond diode lasers (IBH nanoleds) in an IBH Fluorocube apparatus. The emission was collected at a magic-angle polarization using a Hamamatsu MCP photomultiplier (5000U-09). The time-correlated single photon counting (TCSPC) setup consists of an Ortec 9327 CFD and a Tennelec TC 863 TAC. The data were collected with

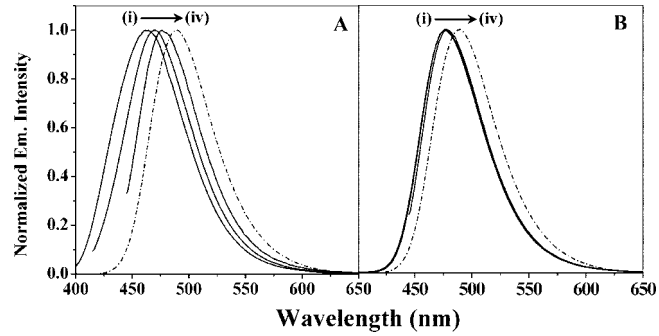

Figure 3. Emission spectra of C480 in 5 wt % P123 when excited at (i) 375, (ii) 405, and (iii) 435 nm and of (iv) C480 in water (—•—) (λ_{ex} = 375−435 nm), in the presence of (A) 0.3 M [pmim][BF_4] and (B) 0.9 M [pmim][BF_4].

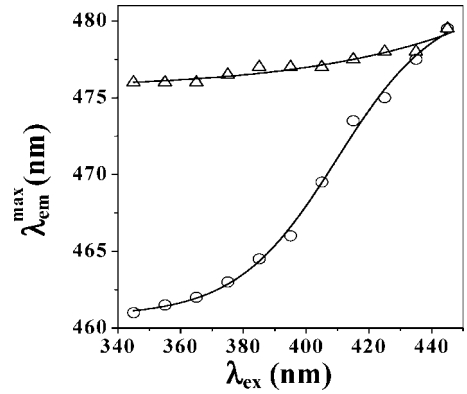

Figure 4. Plot of emission maximum of C480 in 5 wt % P123 as a function of excitation wavelength, in the presence of 0.3 M [pmim][BF_4] (○) and 0.9 M [pmim][BF_4] (△).

TABLE 3: Parameters of Anisotropy Decay of C480 in 5 wt % P123 in the Presence of [pmim][BF_4]

			decay parameters of $r(t)$		
concn of [pmim][BF_4] (mol/L)	λ_{ex} (nm)	r_0	τ_{fast}[a] (ps) (a_{fast})	τ_{slow}[a] (ps) (a_{slow})	$\langle\tau_{rot}\rangle$ (ps)
0	375	0.36	650 (0.30)	3750 (0.70)	2800
	405	0.34	650 (0.25)	3750 (0.75)	3000
	435	0.33	350 (0.40)	2000 (0.60)	1350
0.3	375	0.30	400 (0.25)	2500 (0.75)	1950
	405	0.35	400 (0.35)	2500 (0.65)	1750
	435	0.29	400 (0.55)	2500 (0.45)	1350
0.9	375	0.28	200 (0.30)	800 (0.70)	600
	405	0.31	200 (0.30)	800 (0.70)	600
	435	0.25	200 (0.40)	800 (0.60)	550

[a] Values are ±5%.

a PCA3 card (Oxford) as a multichannel analyzer. The typical fwhm of the system response using a liquid scatterer is about 90 ps. The picosecond fluorescence decays were deconvoluted using IBH DAS6 software. All experiments were done at room temperature (293 K).

The time-resolved emission spectra (TRES) were constructed using the parameters of best fit to the fluorescence decays and the steady state emission spectrum following the procedure described by Maroncelli and Fleming.[20a] The solvation dynamics is described by the decay of the solvent correlation function $C(t)$, defined as

$$C(t) = \frac{\nu(t) - \nu(\infty)}{\nu(0) - \nu(\infty)} \quad (1)$$

where $\nu(0)$, $\nu(t)$, and $\nu(\infty)$ are the emission maxima (frequencies) at time 0, t, and ∞, respectively. Note that a portion of

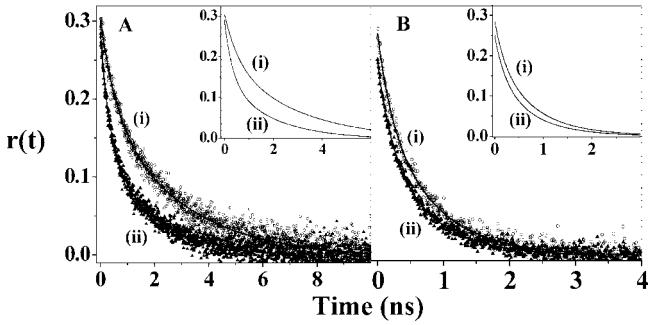

Figure 5. Fluorescence anisotropy decay of C480 in 5 wt % P123 along with fitted curve at (i) $\lambda_{ex} = 375$ nm ($\lambda_{em} = 460$ nm) and (ii) $\lambda_{ex} = 435$ nm ($\lambda_{em} = 460$ nm) in the presence of (A) 0.3 M [pmim][BF_4] and (B) 0.9 M [pmim][BF_4]. Fitted curves of the decays are shown in the inset.

solvation dynamics is missed even in our femtosecond setup of time resolution 350 fs. The amount of solvation missed is calculated using the Fee-Maroncelli procedure.[20b] The emission frequency at time zero, $\nu^{p}_{em}(0)$, may be calculated using the absorption frequency (ν^{p}_{abs}) in a polar medium (i.e., C480 in P123−[pmim][BF_4]) as[20b]

$$\nu^{p}_{em}(0) = \nu^{p}_{abs} - (\nu^{np}_{abs} - \nu^{np}_{em}) \quad (2)$$

where ν^{np}_{em} and ν^{np}_{abs} denote the steady-state frequencies of emission and absorption, respectively, of the probe (C480) in a nonpolar solvent (i.e., cyclohexane).

In order to study fluorescence anisotropy decay, the analyzer was rotated at regular intervals to get perpendicular ($I_\perp$) and parallel ($I_{||}$) components. Then the anisotropy function $r(t)$ was calculated using the formula

$$r(t) = \frac{I_{||}(t) - GI_\perp(t)}{I_{||}(t) + 2GI_\perp(t)} \quad (3)$$

The G value of the picosecond setup was determined using a probe whose rotational relaxation is very fast, (e.g., C480 in methanol), and the G value was found to be 1.5.

The dynamic light scattering studies were carried out in a Nano-ZS instrument (Malvern, U.K.) using a 5 mW He−Ne laser (632 nm).

3. Results and Discussion

3.1. Dynamic Light Scattering Studies. Dynamic light scattering (DLS) data (Table 1, Figure 1) indicate formation of aggregates involving both P123 and [pmim][BF_4]. Addition of [pmim][BF_4] to an aqueous solution containing 5 wt % P123 (∼8.7 mM) causes a slight change in the size of micellar aggregates. In the absence of [pmim][BF_4] the diameter of the P123 micelles is found to be ∼18 nm, which is consistent with previous SANS studies.[15] On addition of [pmim][BF_4], the size of the aggregate slightly increases to 21 nm in 0.3 M RTIL and at the maximum concentration (0.9 M) of [pmim][BF_4] the diameter decreases to 13.5 nm. At a [pmim][BF_4] concentration more than 1 M, the system becomes unstable and phase separation occurs.

The effect of [pmim][BF_4] on the size of P123 micelle is found to be different from the reported effect of [bmim][Br] on P104[14a] or of [pmim][Br] on P123.[14c] An ionic liquid containing Br^- counterion ([bmim][Br] or [pmim][Br]) is highly soluble in water,[14] and it is possible to dissolve more than 3 M in water. In a solution containing 3 M [bmim][Br] and 5 wt % P104, the effective diameter is ∼500 nm.[14a] For 3 M [pmim][Br] and 5 wt % P123, the diameter is ∼3500 nm.[14c] It seems that the main criterion for observing very big clusters (500 or 3500 nm) is high solubility of the ionic liquid in water. This condition is

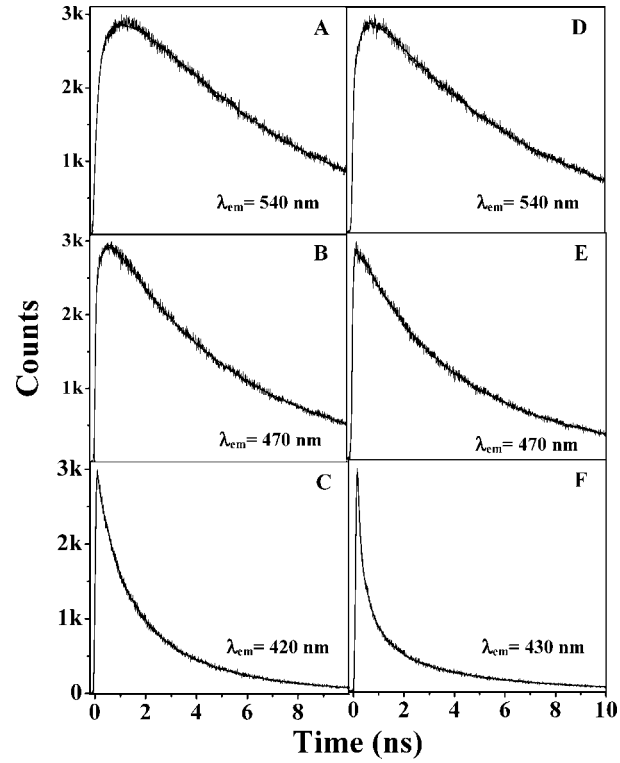

Figure 6. Picosecond decay of C480 ($\lambda_{ex} = 375$ nm) in 5 wt % P123 in the presence of 0.3 M [pmim][BF_4] (A−C) and 0.9 M [pmim][BF_4] (D−F); λ_{em} at (A) 540, (B) 470, (C) 420, (D) 540, (E) 470, and (F) 430 nm.

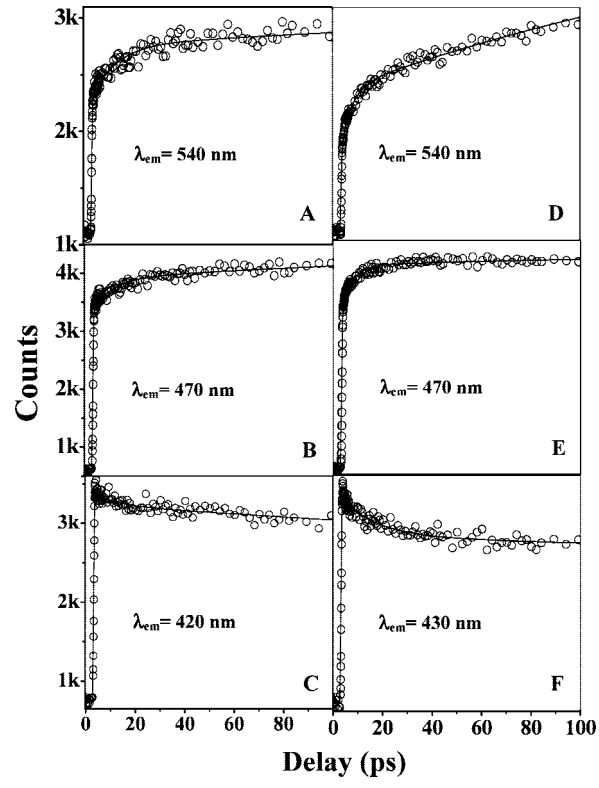

Figure 7. Femtosecond transient of C480 ($\lambda_{ex} = 375$ nm) in 5 wt % P123 in the presence of 0.3 M [pmim][BF_4] (A−C) and 0.9 M [pmim][BF_4] (D−F); λ_{em} at (A) 540, (B) 470, (C) 420, (D) 540, (E) 470, and (F) 430 nm.

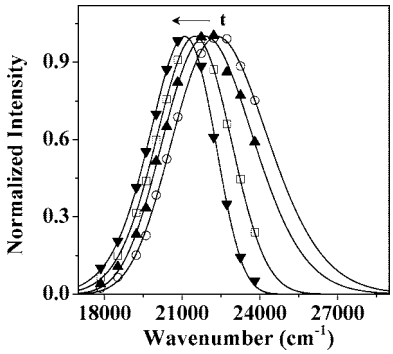

Figure 8. Time-resolved emission spectra (TRES) of C480 ($\lambda_{ex} = 405$ nm) in 5 wt % P123 in the presence of 0.3 M [pmim][BF_4] at 0 (○), 500 (▲), 1000 (□) and 12 000 ps (▼).

satisfied for Br^--containing ionic liquids but not for the sparingly soluble BF_4^--containing ionic liquids (solubility of [pmim][BF_4] in water 0.7 M at 20 °C). The solubility difference also suggests that the ionic liquids containing Br^- are hydrophilic while BF_4^--containing ionic liquids are relatively hydrophobic.

The concentration of [pmim][BF_4] in the mixed micelle is far higher than that of the P123 (5 wt %, i.e., 8.7 mM). The number of [pmim][BF_4] molecules, is ~100 times of that of the P123 molecules at 0.9 M [pmim][BF_4] and about 30 times at 0.3 M. Thus, in the presence of both 0.3 and 0.9 M [pmim][BF_4], the mixed micelle consists of an excess of [pmim][BF_4]. However, it should be pointed out that the molecular weight and size of a P123 molecule is about 24 times that of [pmim][BF_4]. Thus only at >0.3 M [pmim][BF_4] can one say that the volume of the RTIL in the mixed micelle is greater than that of P123.

Incorporation of large number [pmim][BF_4] within P123 affects the structure of the micelle. Obviously, [pmim][BF_4] remains as an ion pair within the P123 micelle and being hydrophobic preferentially goes to the core (PPO block) of the P123 micelle. The presence of a large number of the ion pairs in the core and their electrostatic repulsion may be responsible for the expansion of the core and, hence, the observed slight increase in the size in 0.3 M [pmim][BF_4]. We will see later that at a [pmim][BF_4] concentration more than 0.3 M the corona region is also affected (as evidenced by a decrease in REES discussed below). Thus the nature of the micelle changes above 0.3 M [pmim][BF_4], and this may be the reason for the decrease in the size of the mixed micelle. In the following section, we investigate the effect of addition of [pmim][BF_4] to P123 micelle on the steady state and time-resolved emission spectra of C480.

3.2. Steady State Absorption and Emission Spectra: λ_{ex} Dependence. Penetration of a P123 micelle by the ionic liquid [pmim][BF_4] causes a red shift in the absorption maximum of C480. In a P123 micelle (5 wt %), the absorption maximum of C480 is at 383 nm (Figure 2). This is close to the reported absorption maximum (~380 nm) of C480 in acetonitrile[21] and is blue-shifted by 13 nm from the absorption maximum (396 nm)[21] in water. On addition of 0.3 M [pmim][BF_4], the absorption maximum of C480 undergoes a red shift (Figure 2) to 387 nm. This is close to the reported absorption peak of C480 in ethanol.[21] On addition of 0.9 M RTIL to the P123 solution, the absorption maximum of C480 undergoes a further red shift to 396 nm, which is close to that of C480 in water. This indicates an increase in the local polarity inside the P123 micelles presumably because of the presence of a large number of ion pairs of the RTIL inside the micelle.

The emission maximum (λ_{em}^{max}) of C480 in the P123 micelle depends markedly on the excitation wavelength (λ_{ex}).[16d] The λ_{em}^{max} of C480 exhibits a 25 nm red shift (red edge excitation shift, REES) from 453 nm at $\lambda_{ex} = 345$ nm to 477 nm at $\lambda_{ex} = 435$ nm. This suggests that the PPO core of the P123 micelle (selected at $\lambda_{ex} = 345$ nm) is nearly as polar as acetonitrile ($\lambda_{em}^{max} \sim$ at 453 nm).[21] At $\lambda_{ex} = 435$ nm, the C480 molecules in the hydrophilic PEO corona region are excited and for them λ_{em}^{max} is at 477 nm. This is same as the λ_{em}^{max} of C480 in a 1:1 water−ethanol mixture (477 nm).[21]

On addition of 0.3 M RTIL ([pmim][BF_4]), the λ_{em}^{max} in the core region ($\lambda_{ex} \sim 350$ nm) exhibits a ~8 nm red shift to 461 nm from that in the absence of the RTIL. This indicates penetration of the core by the ion pairs of the RTIL. In 0.3 M RTIL, the corona region ($\lambda_{ex} \sim 440$ nm) is less affected and λ_{em}^{max} exhibits a 2 nm red shift to 480 nm. Thus, on addition of 0.3 M [pmim][BF_4] to 5 wt % P123, the REES (19 nm) is 6 nm less than that (25 nm) in the absence of the RTIL. This once again suggests that, at 0.3 M RTIL, the corona region remains unaffected.

In 0.9 M ([pmim][BF_4]), the REES of C480 in P123 becomes very small (~4 nm). In this case, λ_{em}^{max} shifts from 476 nm at $\lambda_{ex} = 345$ nm to 480 nm at $\lambda_{ex} = 445$ nm. It seems that the IL penetrates even the PPO core as well as the peripheral corona region so that the difference in the polarity of the core and corona region decreases (Table 2). As noted earlier, at 0.9 M RTIL, the total volume of the RTIL inside the mixed micelle is much larger than that of P123 and hence, the nature of the mixed micelle is totally different from that of P123 micelle.

Figure 3 shows the emission spectra of C480 in P123−[pmim]-[BF_4] mixed micelle for 0.3 and 0.9 M RTIL at different excitation wavelengths. Figure 4 shows the corresponding λ_{ex} dependence of λ_{em}^{max} of coumarin 480 for the same systems.

3.3. Fluorescence Anisotropy Decay of C480 in P123−[pmim][BF_4] Micelle. The time constant of fluorescence anisotropy decay of C480 in bulk water is 70 ps.[22] It may be recalled that, in the highly viscous RTIL [pmim][BF_4], the anisotropy decay is much slower (3800 ps).[10] The fluorescence anisotropy decay of C480 in P123 micelle and in P123−[pmim][BF_4] micelle (at the blue side of the emission peak) is found to be much slower and is biexponential:

$$r(t) = r_0[\beta \exp(-t/\tau_{slow}) + (1-\beta) \exp(-t/\tau_{fast})] \quad (4)$$

In a P123 micelle,[18c] at $\lambda_{ex} = 435$ nm which excites the corona region (PEO block), the anisotropy decay is described by two shorter components of 350 ps (40%) and 2000 ps (60%) with $\langle\tau_{rot}\rangle = 1350$ ps. These components are very similar to those obtained for C480 in a Triton X-100 (TX-100) micelle.[18e] Thus the local friction in the corona region of P123 micelles resembles that in TX-100 micelle.

The anisotropy decay of C480 in P123 micelle for $\lambda_{ex} = 375$ nm (i.e., core region) is much slower and exhibits two components, 650 ps (30%) and 3750 ps (70%), with $\langle\tau_{rot}\rangle = 2800$ ps (Table 3).[18c] The slower rotational dynamics at shorter λ_{ex} suggests that inside the P123 micelle the friction in the core is higher than that in the corona region.

As summarized in Table 3, on addition of 0.3 M [pmim][BF_4] to P123, the anisotropy decay of C480 in the corona region ($\lambda_{ex} = 435$ nm) remains unaffected. However, in 0.3 M RTIL/P123, the anisotropy decay in the core ($\lambda_{ex} = 375$ nm) is faster ($\langle\tau_{rot}\rangle = 1950$ ps) than that in the absence of the RTIL. This further suggests that, in 0.3 M [pmim][BF_4], the core is very much affected by penetration of the ionic liquid while the corona region remains more or less similar.

TABLE 4: Decay Parameters of $C(t)$ of C480 in 5 wt % P123 Micelle in the Presence of 0.3 and 0.9 M [pmim][BF4] at Different λ_{ex} Values

λ_{ex} (nm)	$\Delta\nu_{obs}$[a] ($\nu(0)$) (cm^{-1})		decay parameters of $C(t)$, τ_i,[b] a_i (ps)			
			0.3 M [pmim][BF4]		0.9 M [pmim][BF4]	
	0.3 M IL	0.9 M IL		$\langle\tau_s\rangle$		$\langle\tau_s\rangle$
375	1500 (22 700)	890 (21 750)	4 (10%), 200 (35%), 4000 (55%)	2270	<0.3 (30%),[c] 2 (25%), 400(40%), 2000 (5%)	260
405	1250 (22 350)	820 (21 650)	<0.3 (20%),[c] 4 (20%), 200 (30%), 4000 (30%)	1260	<0.3 (40%),[c] 2 (20%), 100 (30%), 2000 (10%)	230
435	300 (21 270)	250 (21 120)	<0.3 (80%),[c] 4 (10%), 200 (10%)	20	<0.3 (80%),[c] 2 (15%), 100 (5%)	5

[a] Values are ±100 cm^{-1}. [b] Values are±10%. [c] Calculated using the Fee−Maroncelli method.[20b]

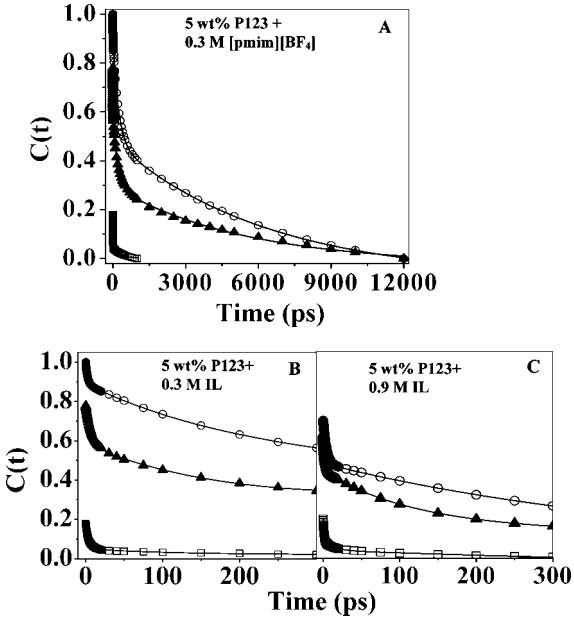

Figure 9. Complete decay of solvent response function $C(t)$ of C480 in 5 wt % P123 in the presence of (A) 0.3 M [pmim][BF_4], λ_{ex} at 375 (○), 405 (▲), and 435 nm (□). The points denote the actual values of $C(t)$, and the solid line denotes the best fit. Initial portions of the decays are shown in (B) 0.3 M [pmim][BF_4] and (C) 0.9 M [pmim][BF_4] for the same excitation wavelengths.

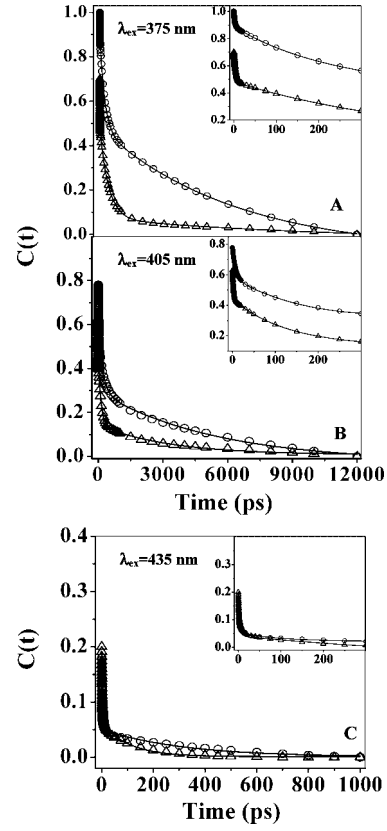

Figure 10. Complete decay of solvent response function $C(t)$ of C480 in 5 wt % P123 for (A) λ_{ex} = 375 nm, (B) λ_{ex} = 405 nm, and (C) λ_{ex} = 435 nm, in the presence of 0.3 M [pmim][BF_4] (○) and 0.9 M [pmim][BF_4] (△). The points denote the actual values of $C(t)$, and the solid line denotes the best fit. Initial portions of the decays are shown in the inset.

In the presence of 0.9 M [pmim][BF_4], both the core and corona are affected and the rotational dynamics shows very small λ_{ex} dependence (Figure 5). In this case, the average rotational relaxation time is 600 ps at λ_{ex} = 375 nm and 550 ps at λ_{ex} = 435 nm. Thus, in 0.9 M ionic liquid, the differences in the friction in the core and the corona are similar. It is apparent that penetration of the entire P123 micelle by RTIL reduces the overall friction.

It is evident that the anisotropy decay in a P123 micelle in the presence of the RTIL (at both 0.3 and 0.9 M) is faster than that in neat RTIL ($\tau_{rot} \sim$ 3800 ps)[10] and in P123 micelle.[18c] The average rotational time (∼600 ps) is similar to that (800 and 100 ps) at the interface of a surfactant (TX-100) and the same RTIL ([pmim][BF_4]) in an ionic liquid containing reverse micelle.[10] It seems the interaction of the RTIL with the surfactant (P123) disentangles the P123 clusters while insertion of the P123 chains within the ionic liquid increases the distance between the ion pairs. Thus the friction in a RTIL/P123 system is less than that in both RTIL alone and P123 micelle.

3.4. Solvation Dynamics of C480 in P123−[pmim][BF_4] Micelle. Figures 6 and 7 show the picosecond and femtosecond transients of C480 in P123 micelle in the presence of 0.3 and 0.9 M [pmim][BF_4]. In an aqueous solution containing [pmim][BF_4] and 5 wt % P123, emission of C480 exhibits a rise at the red end of the emission spectrum and decay at the blue end. This is a clear signature of solvation dynamics.

At λ_{ex} = 375 nm (i.e., for the core region), in the mixed micelle containing 0.3 M [pmim][BF_4] and 5 wt % P123, the fluorescence decay of C480 at 410 nm (blue end) exhibits four decay components: 2, 150, 900, and 3100 ps. At 540 nm (red end), there are three rise components: 10, 400, and 2650 ps, and a long decay component of 5750 ps.

For 0.9 M RTIL and 5 wt % P123, at λ_{ex} = 375 nm, the decay components at λ_{em} = 430 nm are 3, 100, 700, and 3950 ps. In this case, at 530 nm, three rise components (6, 200, and 2450 ps) precede a long decay (5600 ps).

For λ_{ex} = 435 nm (at the corona region), in 0.3 M [pmim][BF_4] and 5 wt % P123, the femtosecond transients of C480 at λ_{em} = 550 nm (red end) display two rise components of 3 and 1350 ps followed by a decay component of 6000 ps. At the blue end (λ_{em} = 450 nm) there are two decay components: 7 and 600 ps, along with a long decay component of 5100 ps.

In 0.9 M ionic liquid/P123 mixed micelle, at λ_{ex} = 435 nm, the femtosecond transient at the red end (λ_{em} = 550 nm) displays

three rise components (3, 300, and 2650 ps) followed by a long decay (5550 ps). In this case, at $\lambda_{em} = 450$ nm, there are three decay components (9, 350, and 1400 ps) and a long decay (4650 ps).

Figure 8 shows the time-resolved emission spectra (TRES) of C480 in a P123−[pmim][BF_4] micelle for $\lambda_{ex} = 405$ nm. From Table 4, it is evident that, on addition of the ionic liquid to P123 micelle, the total dynamic Stokes shift (DSS = $\nu(0) - \nu(\infty)$) decreases 5−4 times as λ_{ex} increases from 375 to 435 nm. This implies that the solvation dynamics becomes faster with increase in λ_{ex}. For $\lambda_{ex} = 375$ nm (i.e., for the core) almost the entire amount of solvation is captured when the concentration of the added RTIL is 0.3 M. However, for 0.9 M ionic liquid, a significant amount of solvation dynamics is missed even in our femtosecond setup at $\lambda_{ex} = 375$ nm. The amount of solvation missed may be calculated by using the Fee−Maroncelli procedure.[20b] Figures 9 and 10 show the decays of the solvent response function, $C(t)$, for different excitation wavelengths, and Table 4 summarizes the decay parameters of $C(t)$ along with DSS.[23]

From Figures 9 and 10 and Table 4, it is evident that, for $\lambda_{ex} = 375$ nm, solvation dynamics in a P123 micelle in the presence of 0.3 M [pmim][BF_4] displays a very fast component (∼4 ps) and a very long component (4000 ps) along with an intermediate component (200 ps). With increase in λ_{ex}, the solvation dynamics becomes faster in both the cases. For $\lambda_{ex} = 435$ nm, in both the systems a major part of solvation dynamics is missed in our femtosecond set up (resolution 0.3 ps) and a 2−4 ps component is detected. In the presence of 0.3 M ionic liquid, the contribution of the ultraslow component decreases gradually from 55% at $\lambda_{ex} = 375$ nm to 30% at $\lambda_{ex} = 405$ nm and finally disappears at $\lambda_{ex} = 435$ nm. The average solvation time is $\langle\tau_s\rangle \sim 2270$ ps at $\lambda_{ex} = 375$ nm and 20 ps at $\lambda_{ex} = 435$ nm.

Similar, sharp acceleration in solvation dynamics with increase in λ_{ex} and complete disappearance of the ultraslow component at $\lambda_{ex} = 435$ nm is also observed in P123 micelle in the presence of 0.9 M ionic liquid (Figure 9 and Table 4). The very fast solvation dynamics in 0.9 M ionic liquid may be attributed to the almost complete absence of the slow core region because of penetration of the ionic liquid. In 0.9 M RTIL and 5 wt % P123, the $\langle\tau_s\rangle$ decreases from 260 ps at $\lambda_{ex} = 375$ nm to 5 ps at $\lambda_{ex} = 435$ nm.

Note that, in the case of neat [pmim][BF_4], with increase in λ_{ex}, the average solvation time decreases from 860 ps at $\lambda_{ex} = 375$ nm to 135 ps at $\lambda_{ex} = 435$ nm.[10]

For $\lambda_{ex} = 405$ nm, the intermediate component in the P123 micelle in the presence of 0.3 M ionic liquid (200 ps) is about 2-fold slower than that in the presence of 0.9 M ionic liquid (100 ps). Many previous experiments and simulations have suggested that such a component arises from polymer chain dynamics.[16,24–26]

The ultraslow component (2000−4000 ps) observed is similar in time scale to those reported for polymer and polymer−surfactant aggregates.[27] The origin of this could be rupture of the water−polymer hydrogen bond of quasi-bound waters as envisaged by Nandi and Bagchi.[28] Such conversion of bound water to free water may also involve coherent motion of the polymer chain ("cooperative chain melting"). The other possible mechanism could be self-diffusion of the probe (C480) molecule from a nonpolar to polar region following excitation. This has been suggested in several recent simulations.[29]

4. Conclusion

This work shows that addition of the ionic liquid [pmim][BF_4] to a P123 micelle affects the structure and dynamics. At a low concentration (0.3 M), the sparingly water soluble ionic liquid preferentially penetrates the hydrophobic core of the P123 micelle. At a high concentration (0.9 M) the ionic liquid invades the entire micelle and the difference between the core and the corona decreases. This is reflected in a lower magnitude of λ_{ex} dependence of emission maximum (REES), anisotropy decay, and solvation dynamics for 0.9 M RTIL. In 0.3 M ionic liquid, the REES is 19 nm, while that at 0.9 M ionic liquid is only 3 nm. Addition of 0.3 M ionic liquid accelerates the anisotropy decay at the core ($\lambda_{ex} = 375$ nm), while that in the peripheral corona remains unaffected. At 0.9 M ionic liquid the average rotational relaxation time in all regions ($\lambda_{ex} = 375-435$ nm) are quite close. Solvation dynamics also exhibits marked λ_{ex} dependence in both 0.3 and 0.9 M ionic liquid. Addition of ionic liquid to the P123 micelle is found to accelerate the solvation dynamics. In the presence of 0.3 M RTIL, the average solvation time decreases ∼100 times from 2270 ps at $\lambda_{ex} = 375$ nm to 20 ps at $\lambda_{ex} = 435$ nm. With increase in λ_{ex} from 375 to 435 nm, in 0.9 M ionic liquid and 5 wt % P123 solution, the average solvation time decreases from 260 to 5 ps. The λ_{ex} dependence provides new and interesting information on spatial variation of spectra and dynamics in an ionic liquid swollen P123 micelle.

Acknowledgment. Thanks are due to Department of Science and Technology, India (Project No. IR/I1/CF-01/2002 and J. C. Bose Fellowship), and Council for Scientific and Industrial Research (CSIR) for generous research support. We thank Professor A. Dasgupta and Mr. T. Sarkar (Calcutta University) for allowing us to use their dynamic light scattering machine. A.A., S.D., D.K.D., U.M., and S.G. thank CSIR for awarding fellowships.

References and Notes

(1) (a) Wang, Y.; Jiang, W.; Yan, T.; Voth, G. A. *Acc. Chem. Res.* **2007**, *40*, 1193. (b) Castner, E. W., Jr.; Wishart, J. F.; Shirota, H. *Acc. Chem. Res.* **2007**, *40*, 1217. (c) Iwata, K.; Okajima, H.; Saha, S.; Hamaguchi, H. *Acc. Chem. Res.* **2007**, *40*, 1174. (d) Samanta, A. *J. Phys. Chem. B* **2006**, *110*, 13704.

(2) (a) Hardacre, C.; Holbrey, J. D.; McMath, S. E. J.; Bowron, D. T.; Soper, A. K. *J. Chem. Phys.* **2003**, *118*, 273. (b) Li, J.; Wang, I.; Fruchey, K.; Fayer, M. D. *J. Phys. Chem. A* **2006**, *110*, 10384.

(3) (a) Huang, X. H.; Margulis, C. J.; Li, Y. H.; Berne, B. J. *J. Am. Chem. Soc.* **2005**, *127*, 17842. (b) Kobrak, M. N. *J. Chem. Phys.* **2006**, *125*, 064502. (c) Jeong, D.; Shim, Y.; Choi, M. Y.; Kim, H. J. *J. Phys. Chem. B* **2007**, *111*, 4920. (d) Bhargava, B. L.; Balasubramanian, S. *J. Chem. Phys.* **2006**, *125*, 219901. (e) Liu, X.; Zhou, G.; Zhang, S.; Wu, G.; Yu, G. *J. Phys. Chem. B* **2007**, *111*, 5658. (f) Ghatee, M. H.; Ansari, Y. *J. Chem. Phys.* **2007**, *126*, 154502. (g) Shim, Y.; Duan, J.; Choi, M. Y.; Kim, H. J. *J. Chem. Phys.* **2003**, *119*, 6411.

(4) (a) Pal, A.; Samanta, A. *J. Phys. Chem. B* **2007**, *111*, 4724. (b) Paul, A.; Mandal, P. K.; Samanta, A. *J. Phys. Chem. B* **2005**, *109*, 9148. (c) Mandal, P. K.; Sarkar, M.; Samanta, A. *J. Phys. Chem. A* **2004**, *108*, 9048. (d) Karmakar, R.; Samanta, A. *J. Phys. Chem. A* **2002**, *106*, 6670. (e) Karmakar, R.; Samanta, A. *J. Phys. Chem. A* **2002**, *106*, 4447.

(5) (a) Jin, H.; Baker, G. A.; Arzhantsev, S.; Dong, J.; Maroncelli, M. *J. Phys. Chem. B* **2007**, *111*, 7291. (b) Arzhantsev, S.; Jin, H.; Baker, G. A.; Maroncelli, M. *J. Phys. Chem. B* **2007**, *111*, 4978. (c) Ito, N.; Arzhantsev, S.; Heitz, M.; Maroncelli, M. *J. Phys. Chem. B* **2004**, *108*, 5771. (d) Ito, N.; Arzhantsev, S.; Maroncelli, M. *Chem. Phys. Lett.* **2004**, *396*, 83. (e) Ingram, J. A.; Moog, R. S.; Ito, N.; Biswas, R.; Maroncelli, M. *J. Phys. Chem. B* **2003**, *107*, 5926.

(6) (a) Funston, A. M.; Fadeeva, T. A.; Wishart, J. F.; Castner, E. W., Jr. *J. Phys. Chem. B* **2007**, *111*, 4963. (b) Shirota, H.; Castner, E. W., Jr. *J. Phys. Chem. B* **2007**, *111*, 4819. (c) Shirota, H.; Funston, A. M.; Wishart, J. F.; Castner, E. W., Jr. *J. Chem. Phys.* **2005**, *122*, 184512.

(7) (a) Wang, Y.; Voth, G. A. *J. Am. Chem. Soc.* **2005**, *127*, 12192. (b) Bhargava, B. L.; Devane, R.; Klein, M. L.; Balasubramanium, S. *Soft Matter* **2007**, *3*, 1395. (c) Lopes, J. N. A. C.; Padua, A. A. H. *J. Phys. Chem. B* **2006**, *110*, 3330. (d) Hu, Z.; Margulis, C. J. *Proc. Natl. Acad. Sci. U.S.A.* **2006**, *103*, 831.

(8) (a) Triolo, A.; Russina, O.; Bleif, H.-J.; Di Cola, E. *J. Phys. Chem. B* **2007**, *111*, 4641. (b) Xiao, D.; Rajian, J. R.; Cady, A.; Li, S.; Bartsch, R. A.; Quitevis, E. L. *J. Phys. Chem. B* **2007**, *111*, 4669.

(9) (a) Shigeto, S.; Hamaguchi, H. *Chem. Phys. Lett.* **2006**, *427*, 329. (b) Katayanagi, H.; Hayashi, S.; Hamaguchi, H.; Nishikawa, K. *Chem. Phys. Lett.* **2004**, *392*, 460.

(10) Adhikari, A.; Sahu, K.; Dey, S.; Ghosh, S.; Mandal, U.; Bhattacharyya, K. *J. Phys. Chem. B* **2007**, *111*, 12809.

(11) (a) Chowdhury, P. K.; Halder, M.; Sanders, L.; Calhoun, T.; Anderson, J. L.; Armstrong, D. W.; Petrich, J. W. *J. Phys. Chem. B* **2004**, *108*, 10245. (b) Mukherjee, P.; Crank, J. A.; Halder, M.; Armstrong, D. W.; Petrich, J. W. *J. Phys. Chem. A* **2006**, *110*, 10725. (c) Seth, D.; Chakraborty, A.; Setua, P.; Sarkar, N. *J. Phys. Chem. B* **2007**, *111*, 4781. (d) Chakraborty, A.; Seth, D.; Chakrabarty, D.; Setua, P.; Sarkar, N. *J. Phys. Chem. A* **2005**, *109*, 11110. (e) Seth, D.; Chakraborty, A.; Setua, P.; Sarkar, N. *Langmuir* **2006**, *22*, 7768.

(12) (a) Gao, Y.; Li, N.; Zheng, L.; Bai, X.; Yu, L.; Zhao, X.; Zhang, J.; Zhao, M.; Li, Z. *J. Phys. Chem. B* **2007**, *111*, 2506. (b) Gao, H.; Li, J.; Han, B.; Chen, W. L.; Zhang, J.; Zhang, R.; Yan, D. *Phys. Chem. Chem. Phys.* **2004**, *6*, 2914. (c) Eastoe, J.; Gold, S.; Rogers, S. E.; Paul, A.; Welton, T.; Heenan, R. K.; Grillo, I. *J. Am. Chem. Soc.* **2005**, *127*, 7302.

(13) (a) Sando, G. M.; Dahl, K.; Owrutsky, J. C. *J. Phys. Chem. B* **2007**, *111*, 4901. (b) Sando, G. M.; Dahl, K.; Owrutsky, J. C. *Chem. Phys. Lett.* **2006**, *418*, 402.

(14) (a) Zheng, L.; Guo, C.; Wang, J.; Liang, X.; Chen, S.; Ma, J.; Yang, B.; Jiang, Y.; Liu, H. *J. Phys. Chem. B* **2007**, *111*, 1327. (b) Seddon, K. R.; Stark, A.; Torres, M. J. *Pure Appl. Chem.* **2000**, *72*, 2275. (c) Dey, S.; Adhikari, A.; Das, D. K.; Bhattacharyya, K. Unpublished.

(15) (a) Mortensen, K. *Macromolecules* **1997**, *30*, 503. (b) Goldmints, I.; von Gottberg, K.; Smith, K. A.; Hatton, T. A. *Langmuir* **1997**, *13*, 3659. (c) Wanka, G.; Hoffmann, H.; Ulbricht, W. *Macromolecules* **1994**, *27*, 4145. (d) Hecht, E.; Mortensen, K.; Gradzielski, M.; Hoffmann, H. *J. Phys. Chem.* **1995**, *99*, 4866. (e) Ganguly, R.; Aswal, V. K.; Hassan, P. A.; Gopalakrishnan, I. K.; Kulshreshtha, S. K. *J. Phys. Chem. B* **2006**, *110*, 9843.

(16) (a) Humpolickova, J.; Stepanek, M.; Prochazka, K.; Hof, M. *J. Phys. Chem. A* **2005**, *109*, 10803. (b) Grant, C. D.; DeRitter, M. R.; Steege, K. E.; Fadeeva, T. A.; Castner, E. W., Jr. *Langmuir* **2005**, *21*, 1745. (c) Grant, C. D.; Steege, K. E.; Bunagan, M. R.; Castner, E. W., Jr. *J. Phys. Chem. B* **2005**, *109*, 22273. (d) Sen, P.; Ghosh, S.; Sahu, K.; Mondal, S. K.; Bhattacharyya, K. *J. Chem. Phys.* **2006**, *124*, 204905. (e) Mali, K. S.; Dutt, G. B.; Mukherjee, T. *J. Chem. Phys.* **2006**, *124*, 054904.

(17) (a) Demchenko, A. P. *Biophys. Chem.* **1982**, *15*, 101. (b) Demchenko, A. P. *Luminescence* **2002**, *17*, 19. (c) Lakowicz, J. R. *Biochemistry* **1984**, *23*, 3013. (d) Kelkar, D. A.; Chattopadhyay, A. *J. Phys. Chem. B* **2004**, *108*, 12151. (e) Mukherjee, S.; Chattopadhyay, A. *Langmuir* **2005**, *21*, 287.

(18) (a) Satoh, T.; Okuno, H.; Tominaga, K.; Bhattacharyya, K. *Chem. Lett.* **2004**, *33*, 1090. (b) Sen, P.; Satoh, T.; Bhattacharyya, K.; Tominaga, K. *Chem. Phys. Lett.* **2005**, *411*, 339. (c) Mandal, U.; Adhikari, A.; Dey, S.; Ghosh, S.; Mondal, S. K.; Bhattacharyya, K. *J. Phys. Chem. B* **2007**, *111*, 5896. (d) Ghosh, S.; Adhikari, A.; Mandal, U.; Dey, S.; Bhattacharyya, K. *J. Phys. Chem. C* **2007**, *111*, 8775. (e) Ghosh, S.; Mondal, S. K.; Sahu, K.; Bhattacharyya, K. *J. Chem. Phys.* **2007**, *126*, 204708.

(19) (a) Namboodiri, V. V.; Varma, R. S. *Org. Lett.* **2002**, *4* (18), 3161. (b) Ding, S.; Radosz, M.; Shen, Y. *Macromolecules* **2005**, *38*, 5921. (c) Dupont, J.; Consorti, C. S.; Suarez, P. A. Z.; de Souza, R. F. *Org. Synth.* **2004**, *10*, 184.

(20) (a) Maroncelli, M.; Fleming, G. R. *J. Chem. Phys.* **1987**, *86*, 6221. (b) Fee, R. S.; Maroncelli, M. *Chem. Phys.* **1994**, *183*, 235.

(21) Jones, G., II; Jackson, W. R.; Choi, C.-Y.; Bergmark, W. R. *J. Phys. Chem.* **1985**, *89*, 294.

(22) (a) Shirota, H.; Segawa, H. *J. Phys. Chem. A* **2003**, *107*, 3719. (b) Shirota, H. *J. Phys. Chem. B* **2005**, *109*, 7053.

(23) We have also estimated the amount of solvation missed by using the ν_{md} defined as $\nu_{md} = (\nu_+ + \nu_-)/2$ at $t = 0$ and $t = \infty$. We found that for $\lambda_{ex} = 375$, 405, and 435 nm the amount of solvation missed is respectively 0%, 25%, and 85% for 0.3 M ionic liquid. This is quite close to the amount of solvation missed using the peak frequency (0%, 20%, and 90%). For 0.9 M ionic liquid, the amount of solvation missed is 30%, 40%, and 80% when we use the peak frequencies while it is 40%, 50%, and 85% using the ν_{md}.

(24) (a) Shirota, H.; Tamoto, Y.; Segawa, H. *J. Phys. Chem. A* **2004**, *108*, 3244. (b) Corbeil, E. M.; Riter, R. E.; Levinger, N. E. *J. Phys. Chem. B* **2004**, *108*, 10777. (c) Tan, H.-S.; Piletic, I. R.; Riter, R. E.; Levinger, N. E.; Fayer, M. D. *Phys. Rev. Lett.* **2005**, *94*, 057405.

(25) (a) Olander, R.; Nitzan, A. *J. Chem. Phys.* **1995**, *102*, 7180. (b) Argaman, R.; Huppert, D. *J. Phys. Chem. A* **1998**, *102*, 6215. (c) Pant, D.; Levinger, N. E. *Langmuir* **2000**, *16*, 10123.

(26) (a) Pal, S. K.; Peon, J.; Bagchi, B.; Zewail, A. H. *J. Phys. Chem. B* **2002**, *106*, 12376. (b) Srinivas, G.; Sebastian, K. L.; Bagchi, B. *J. Chem. Phys.* **2002**, *116*, 7276.

(27) (a) Frauchiger, L.; Shirota, H.; Uhrich, K. E.; Castner, E. W., Jr. *J. Phys. Chem. B* **2002**, *106*, 7463. (b) Sen, S.; Sukul, D.; Dutt, P.; Bhattacharyya, K. *J. Phys. Chem. B* **2002**, *106*, 3763.

(28) (a) Nandi, N.; Bagchi, B. *J. Phys. Chem. A* **1997**, *101*, 10954. (b) Nandi, N.; Bagchi, B. *J. Phys. Chem. B* **1998**, *102*, 8217.

(29) (a) Thompson, W. H. *J. Chem. Phys.* **2004**, *120*, 8125. (b) Gomez, J. A.; Thompson, W. H. *J. Phys. Chem. B* **2004**, *108*, 20144. (c) Mitchell-Koch, K. R.; Thompson, W. H. *J. Phys. Chem. C* **2007**, *111*, 11991. (d) Feng, X.; Thompson, W. H. *J. Phys. Chem. C* **2007**, *111*, 18060. (e) Faeder, J.; Ladanyi, B. M. *J. Phys. Chem. B* **2005**, *109*, 6732. (f) Harpham, M. R.; Ladanyi, B. M.; Levinger, N. E. *J. Phys. Chem. B* **2005**, *109*, 16891. (g) Faeder, J.; Ladanyi, B. M. *J. Phys. Chem. B* **2001**, *105*, 11148.

JP7118857